Production of lignin-containing cellulose nanofibrils by the combination of different mechanical processes

Malek Khadraoui, Ramzi Khiari, Latifa Bergaoui, Evelyne Mauret

Production of lignin-containing cellulose nanofibrils by the combination of different mechanical processes

Malek Khadraoui[a,b], Ramzi Khiari[a,c,d*], Latifa Bergaoui[b], Evelyne Mauret[a]

[a] Univ. Grenoble Alpes, CNRS, Grenoble INP, LGP2, F-38000 Grenoble, France

[b] Carthage University, National Institute of Applied Sciences and Technology, EcoChimie Laboratory, Tunis, Tunisia

[c] University of Monastir, Faculty of Sciences of Monastir, Laboratory of Environmental Chemistry and Clean Process (LCE2P- LR21ES04), 5019 Monastir, Tunisia

[d] Higher Institute of Technological Studies of Ksar Hellal, Department of Textile, Ksar Hellal, Tunisia

*Corresponding author. Email: khiari_ramzi2000@yahoo.fr;

Abstract

Due to its interesting properties, attention has been oriented to the production of cellulose nanofibrils. However, the cellulose isolation requires the combination of several steps which are generally very energy consuming. This is one of the main limitations for the use and industrialisation of such materials. Trying to participate in the resolution of this probleme, lignin-containing cellulose nanofibrils are produced for the first time from *Posidonia oceanica* waste. Fibres are alkali-extracted by a conventional soda cooking in autoclave or by alkaline steam explosion. As conventional refining of unbleached fibres is difficult, a comparative study is carried out to test alternative processes for fibre fibrillation (twin-screw extrusion (1 pass) or steam explosion (during 3 times)). Actually, these two processes are known to be environmentally friendly and low energy consuming. For microfibrillation, an ultra-fine friction grinder is used to prepare lignin-containing cellulose nanofibrils. The obtained gels are characterized by several properties such as morphological analysis (Morfi,

optical microscopy, scanning electron microscopy, transmission electron microscopy) and turbidity measurements. Papers and nanopapers are prepared by filtration to investigate the mechanical properties. All these analysis methods allow discussing the efficiency of the different processcombinations. It is concluded that steam explosion could be an alternative method for *Posidona* fibre extraction, while for refining the process conditions should be optimized. Finally, it is found that LCNF produced from extruded pulps (whatever the fibre extraction method) exhibit promising properties comparing with other unbleached CNF.

Keywords: *Posidonia oceanica*, steam explosion, ultra-fine friction grinder, twin-screw extrusion**.**

ABBREVIATIONS

- U-POB: Unbleached (U) raw fibres of *Posidonia* balls (POB);
- U-POB-A: Extracted fibres by autoclave (A) from *Posidonia* balls;
- U-POB-SE: Extracted fibres by steam explosion (SE) from *Posidonia* balls;
- U-POB-A-TSE: Extracted (autoclave) and extruded (TSE) fibres from *Posidonia* balls;
- U-POB-SE-TSE: Extracted (steam explosion) and extruded fibres from *Posidonia* balls;
- U-POB-A-SE: Extracted (autoclave) and steam exploded fibres from *Posidonia* balls;
- U-POB-SE-SE: Extracted (steam explosion) and steam exploded fibres from *Posidonia* balls;
- U-POB-A-TSE-M: Extracted (autoclave), extruded and grinded (M) fibres from *Posidonia* balls;
- U-POB-SE-TSE-M: Extracted (steam explosion), extruded and grinded fibres from *Posidonia* balls;
- U-POB-A-SE-M: Extracted (autoclave), steam exploded and grinded fibres from *Posidonia* balls;

- U-POB-SE-SE-M: Extracted (stea explosion), steam exploded and grinded fibres from *Posidonia* balls.

1. Introduction

Nowadays, bio-based products are increasingly used in order to replace petroleum-based materials. That is why the interest in cellulose and nanocellulose keeps growing. The properties of cellulosic nanomaterials mainly depend on their specific surface area, aspect ratio and chemical composition (Wagner et al., 2020). By using different approaches, nanocellulose can be produced from various raw materials. Generally speaking, cellulose nanocrystals (CNC) are produced by acid hydrolysis while intense mechanical disintegration leads to cellulose nanofibrils (CNF), also called cellulose microfibrils (CMF). Nevertheless, in recent years, efforts have been directed to develop lignin-containing cellulose nanofibrils (LCNF). Different feedstocks were used such as empty palm fruit bunches (Ago et al., 2016), wheat straw (Espinosa et al., 2016; Sánchez et al., 2016), triticale straw (Tarrés et al., 2017), bamboo chips (Lu et al., 2018) and sunflower stalks (Ewulonu et al., 2019). These nanomaterials, with different lignin contents, can be used in several areas: additives in papermaking (Delgado-Aguilar et al., 2016); composites (Horseman et al., 2017); 3D printing (Chinga-Carrasco et al., 2018) or reinforcing fillers in matrices (Ago et al., 2016; Ferrer et al., 2016; Visanko et al., 2017). Solala et al. (2020) suggested to use the term "lignin-containing cellulose nanofibrils" to refer to all cellulose nanofibrils with a width of less than 100 nm and a lignin content above 1%. One of the pioneering research studies (Wang et al., 2012) used an acid hydrolysis treatment followed by homogenization (high pressure of 60 MPa, 20 passes) to produce LCNF from unbleached kraft wood pulp. These materials, with 5-10% of lignin, exhibited hydrophobic properties, and thus good compatability to polymer matrix for composite applications.

As part of a review on LCNF, Solala et al. (2020) enlightened that lignin can have two contradictory effects on pulp microfibrillation. Some of the researchers reported that lignin hinders microfibrillation, for instance in the case of mechanical pulps (Hanhikoski et al., 2016; Lahtinen et al., 2014). Having a complex, cross-linked structure, lignin appears to inhibit fibre swelling and microfibrillation by locking individual microfibrils. In other works, it was observed that energy consumption can be reduced by the presence of low amounts of lignin in unbleached chemical pulps (Spence et al., 2010). Furthermore, Rojo et al. (2015) and Solala et al. (2012) reported the formation of finer LCNF at comparable energy consumption with the presence of lignin (content between 2% and 14%). This phenomenon was attributed to the amourphous nature of lignin, its capacity to stabilize radicals and the higher electrical charge density of unbleached pulps (Ferrer et al., 2012).

Based on literature, LCNF thus present interesting properties in the field of bioproduct engineeering, due to their lower cost compared to bleached CNF. Indeed, lignin-containing cellulose nanofibrils are produced with minimal chemical pretreatments by eliminating the bleaching step (Osong et al., 2013) and simplifying the manufacture process. Moreover, compared to lignin-free CNF, LCNF nanopapers have much higher hydrophobicity and thermal stability. Previous studies reported that lignin may help improving the CNF nanopapers moisture barrier properties due to lignin hydrophobicity. The hydrophobic character of lignin makes it possible to produce LCNF with good compatibility with hydrophobic matrices leading to a more pronounced reinforcing effect. In addition, as reported by Rojo et al. (2015), nanopapers prepared from LCNF, with high residual lignin content, have smooth surface, with a reduced number and size of micropores leading to a less porous and more compact structure. This may affect their oxygen barrier properties. Therefore, when comparing with bleached CNF, lignin-containing cellulose nanofibrils can be

interesting bio-based alternatives to oil-derived synthetic polymer materials (Solala et al., 2020).

Mainly, two routes are carried out for the production of LCNF. A combination of chemical pretreatment (e.g. TEMPO-oxidation) and mechanical processes (Delgado-Aguilar et al., 2016; Ehman et al., 2020; Herrera et al., 2018; Wen et al., 2019) or a combination of mechanical processes (Rojo et al., 2015; Yousefi et al., 2018).

Adapting these strategies to our work, *Posidonia oceanica* balls were used as raw materials to produce cellulose nanofibrils with high lignin content. *Posidonia* waste, accumulated on the tunisian coasts of the Mediterranean sea, is an abundant and inexpensive raw material and its potential is largely under-exploited for value-added products and applications. Currently, it is mainly burned for energy production after cleaning the beaches for tourism reasons. Few articles have studied the valorization of this specific biomass through the production of bleached cellulosic nanomaterials (Benito-González et al., 2019; Bettaieb et al., 2015; Fortunati et al., 2015, Khadraoui et al., 2022). Our objective is to use unbleached *Posidonia* fibres, pretreated mechanically (by twin-screw extrusion (TSE) or steam explosion (SE)), before ultrafine grinding for microfibrillation.

Twin-screw extrusion and steam explosion are proposed as alternative processes for replacing refining (fibrillation step), which was not feasible for unbleached pulp of *Posidonia.*

Actually, TSE is a thermomechanical process based on two spinning screws rotating in a temperature-controlled barrel. Kneading blocks, reverse and conveying screws are the main elements of the extruder. When processed, the material is transported and submitted to shear forces between the screws and the barrel. Previous studies have reported that the design of screw elements is a key paramater to control the effects of extrusion (Duque et al., 2017). When applied to lignocellulosic biomass, TSE can have effects similar to conventional pulp refining. Chen et al. (2014) have thus shown that extrusion mainly leads to a reduction in

123 particle size and an increase of specific surface area of rice straw. Ämmälä et al. (2019) also
124 reported the effectiveness of extrusion in reducing particle size, leading to the separation of
125 fibres bundles, fibre and fines. It was suggested that kneading elements were behind the
126 extensive fibre shortening, concluding that twin-screw extruder can be used for extracting
127 fibres from wood chips (Hietala et al., 2011). Leu and Zhu (2013) classified the mechanical
128 effects on biomass into two classes: refining I and refining II. Refining I has moderate effects,
129 leading to an increase in the outer surface of the elements by cutting, breaking and
130 disintegrating the fibre bundles and by slightly fibrillating the fibre surface. Refining II is
131 more intense and leads to cell wall breaking. At this stage, extrusion may result in the internal
132 fibrillation of the vegetal fibres and also reduce their size to the micro- or nanoscale by
133 separating the microfibrils in the cell wall. These phenomena are particularly influenced by
134 the configuration of the screws, as high stresses/shear forces are required for a such intense
135 treatment. In this context, Rol et al. (2017) reported the production of cellulose nanofibrils at
136 high solid contents (20%) by combining enzymatic pretreatment or TEMPO-oxidation and
137 twin-screw extrusion.
138 Regarding steam explosion the main advantage is the low energy consumption, due to short
139 processing time (Sui and Chen, 2014) and it can be considered as green process when it was
140 used without toxic reagent. This thermo-mechano-chemical process allows the destructuration
141 of lignocellulosic material by the combination of heat from water steam, polysacharride
142 hydrolysis due to the formation of organic acids and shear resulting from the vaporisation of
143 water in the fibres during depressurization (Overend et al., 1987). This process comprises two
144 stages: steam cracking and explosive decompression. Steam cracking consists in the
145 penetration of water into the material in the form of steam under high pressure and at a high
146 temperature (Avella and Scoditti, 1998). This action induces the hydrolysis of acetyl groups.
147 Thereafter, there will be a release of organic acids (acetic and uronic) leading to the catalysis

of the depolymerization of hemicellulosic fractions (Sun et al., 2005). It has been shown that the application of severe conditions leads to hydrolysis of the cellulosic fraction and degradation of the xylans and glucans formed into furfural and 5-hydroxymethylfurfural (Sun et al., 2005). Morover, several chemicals reagents can also be used at this stage to modify the pH and/or to facilitate the biomass processing , etc. Generally, these treatments, when carried out in alkaline or organic solvents, lead to an increase in the solubility of lignin while keeping cellulose (solid residue) with reduced degree of polymerization (DP). The literature has shown that the efficiency of the steam explosion is intrinsically related not only to residence time and pressure (severity factor) but also to the explosion power density (EPD) which is related to the deflation time during explosion process (Yu et al., 2012). During the second stage called "explosive decompression", the wet saturated lignocellulosic material "bursts" as a result of the sudden release of pressure in the reactor. It was shown that the pressure difference between the inside of the reactor and atmospheric pressure is proportional to the intensity of the shear forces applied to the biomass (Sun et al., 2005). At this phase, re-evaporation of a part of the water condensed in the biomass takes place and thermal energy is converted into mechanical energy (Yu et al., 2012). Shear forces were induced and applied to the material leading to the breakage of cell wall internal structure (Holtzapple et al., 1989). For instance, exploded wood has greater porosity and higher specific surface area (Holtzapple et al., 1989; Qin and Chen, 2015). The study of Tanahashi et al. (1983) proved the appearance of cellulosic fibre substructures, i.e. formation of microfibrils. Increase in fine content coupled with reduction in length of the fibres also occurs for Luo et al. (2018). Some observed fractures are due to degradation of cellulose during the steam explosion. Vignon et al. (1995) treated hemp fibres at 240°C. Apart from some intact fibres, disintegration of the samples into small particles was reported. The scanning electron micrographs show that the higher the temperature, the more the fibres appear separated. Also, Sauvageon et al. (2018)

showed that by increasing the severity conditions, a significant decrease of hemp fibre length and a high content in short fibres (< 3 mm) were observed. Boonterm et al. (2016) studied the effect of increasing pressure and concluded that increasing the pressure from 13 to 15 bar significantly reduced the rice straw fibre diameters for a higher aspect ratio. At 17 bar, the aspect ratio decreased due to significant damage of the fibres. Deepa et al. (2011) and Diop et al. (2015) observed simliar tendencies.

The history of the use of these two processes (TSE and SE) to treat lignocellulosic material, either conventional (wood) or alternative (non-wood and waste materials), lead us to propose their application as pretreatments in the CNF production chain for fibre processing, the objective being to facilitate their further microfibrillation. In fact, the refining of unbleached *Posidonia* was not feasible. This behaviour was observed before in a previous work in our team (Khiari, 2010) and it was not explained. Probably extracted unbleached fibres present lower fibre charge and lower conformability than bleached one. PFI mill seems to be a harsh process for unbleached *Posidonia*. To resolve this probleme, we suggested to use an alternative process, twin-screw extrusion and steam explosion. A comparative study is realized to compare the efficiency of these two processes in the aim of refining (fibrillation) of unbleached *Posidonia* pulps.

This work first focuses on pulping of unbleached *Posidonia* either by alkaline steam explosion or conventional alkaline cooking in autoclave. Then, it has been proposed to replace the conventional refining operation by twin-screw extrusion or steam explosion (in specific conditions). The obtained alkali-treated pulps are thus pretreated to reduce fibre size and promote fibrillation, before the main mechanical process which is grinding. Finally, to investigate the impact of the different routes, morphological properties of suspensions and mechanical properties of prepared papers and nanopapers (elastic modulus) are discussed.

2. Material and methods

2.1 Fibre extraction: Alkali-treatment by autoclave or steam explosion

Posidonia oceanica balls (POB), a marine biomass, were collected in Monastir, on the Tunisian Mediterranean coast. They were washed, air-dried and ground by a ball mill. For pulping, chemicals were used as received from suppliers: sodium hydroxide (NaOH, ≥97%, pellets, Sigma-Aldrich), anthraquinone ($C_{14}H_8O_2$, ≥97%, powder, Sigma-Aldrich).

Electrically-heated rotating autoclaves, located in LGP2, Grenoble (France), are used for fibre extraction. In each reactor, 60 g of ground seagrass (length around 1.7 mm) are disersed in water with 20% of NaOH (w/w, based on dry material, liquor to solid ratio fixed at 10) and 0.1% (w/w, based on dry material) of anthraquinone. Cooking is performed at 160°C for 120 minutes and the reaction is stopped by sprinkling cold water on reactors and degassing. To recover the extracted fibres (U-POB-A), the resulting suspension is washed and filtered with a nylon sieve of 40 μm mesh size (Khiari et al., 2010, 2011).

The apparatus, (designed by LERMaB and ADF) is composed of three main parts: a steam generator, a reactor, and a discharge tank. 150 g of dry ground *Posidonia* are dispresed in water with 10% NaOH with a liquid/solid ratio equal to 10 (w/w, based on dry material). The reactor is pre-heated to the target operating temperature/pressure: 210°C/18 bar. Then, the soaked biomass is loaded into the reactor (without filtration) and heated to the set temperature by steam injection. After a residence time of 6 minutes, the pressure is suddenly released, the seagrass is then ejected from the reactor and recovered in the discharge tank. To recover the extracted fibres (U-POB-SE), the resulting suspension is washed and filtered with a nylon sieve of 40 μm mesh size.

2.2 Mechanical pretreatments: twin-screw extrusion and steam explosion

The fibres extracted by alkaline pulping in autoclave (U-POB-A) or by alkaline steam explosion (U-POB-SE) are pre-treated either by twin-screw extrusion (speed: 1000 rpm; 1

pass) or steam explosion again (temperature/pressure: 200°C/14.5 bar; residence time: 2 minutes performed 3 times). TSE and SE are performed at around 20% (w/w) consistency.

- ***Twin-screw extrusion:*** Twin-screw extrusion is carried out in a Thermo Scientific HAAKE Rheomex OS PTW 16 + HAAKE PolyLab OS RheoDrive 7. This device is equipped with 640 mm long and 16 mm diameter screw. The screw profile was previously optimized by Rol et al. (2020), but for a different purpose i.e. CNF production at high solid content. It comprises 6 kneading zones with reverse rotating elements. The pulp is fed by hand by maintaining a constant flow rate (average dry mass flow of 250 g/h). The screw speed and temperature are maintained at 1000 rpm and 10°C (by a water-cooling system), respectively. The pulp is passed only once.
- ***Steam explosion:*** Steam explosion is also used as a pretreatment. The objective of these trials is to study the impact of depressurization and to assess if it induces a sufficient breakage of the fibre cell wall to promote the subsequent step, i.e. grinding. For this reason, pulps at 10% (w/w) are treated in water for a shorter residence time in the reactor (2 min) but at higher pressure (200°C/14.5 bar). As previously mentioned, ejected fibres are recovered in the discharge tank and filtered using a nylon sieve of 40 µm mesh size. This treatment is repeated 3 times.

2.3 LCNF production by ultrafine grinding

LCNF are produced by using an ultra-fine friction grinder, refered as M, (model MKZA6-2, disc model MKG-C 80, Masuko Sangyo Co., Ltd., Japan). Extracted and pre-treated (TSE ou SE) lignocellulosic fibres are microfibrillated at a concentration of 2%, with a disc rotation velocity between 950 and 1500 rpm. Grinding was first carried out in contact mode (Gap 0 for 5 passes). Then, the gap between the disks is progressively decreased (Gap -5 for 5 passes and -10 for 15 passes) for a total number of 25 passes. To gain a better understanding of the effect

of grinding, samples are taken after every 5 passes (called cycle or zone). Specific energy consumption (kWh/t) is calculated for each cycle as following:

$$\text{Energy consumption of grinding (kWh/t)} = \frac{(P_{tot} - P_{tot,0}) * t_i}{m_i} \quad \text{Eq.1}$$

where P_{tot} is the average power consumption (kW), $P_{tot,0}$ the no-load power (the power consumption of the empty grinder kW), t_i the grinding time (h) and m_i the dry mass of fibres ($t: tons$).

Figure 1 illustrates the different routes studied in this work.

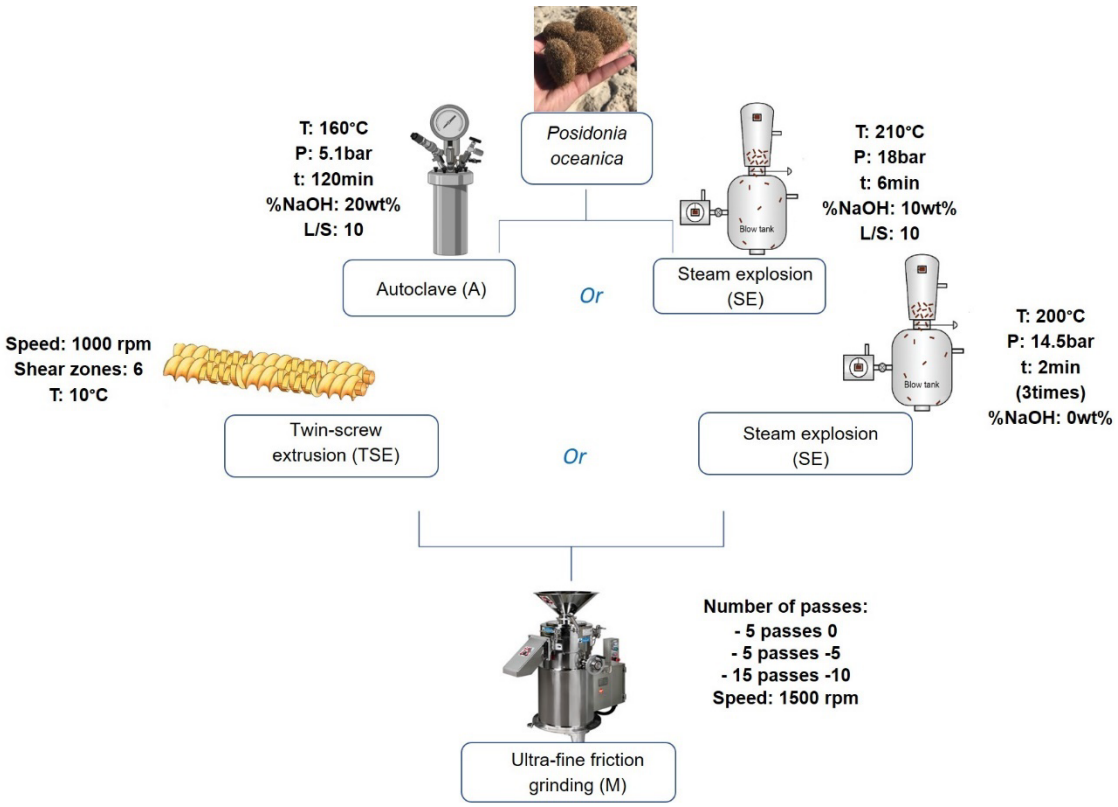

Figure 1. Schematic diagram of the proposed experiments.

2.4 Chemical composition of pulps

The method adopted for the determination of lignin content is the Klason lignin extraction. Prior to the the hyrolysis, the dry biomass is ground and extracted in a toluene/ethanol

mixture with a volume ratio of 2. The extractive free biomass (0.175 g) is treated with 1.5 ml of 72% sulfuric acid at 30°C for one hour. The samples, diluted with 42 mL of deionized water, are heated in the autoclave at 121°C for two hours. After cooling and filtration, the obtained solid fraction is dried (at 105°C for 24 hours) and weighed to calculate Klason lignin content. This mesurement is realized according to the TAPPI standard T-22 om-88 method. The monomer sugar content is determined by the analysis of the filtrate diluted using an ion-exchange chromatography (ICS-3000 Dionex).

2.5 Production and characterization of papers and nanopapers

In order to prepare papers and nanopapers, 2 g (of the dry matter) are dispersed and diluted with deionized water to 0.5% (w/w) and stirred for 30 minutes under magnetic stirring. Then, the suspension is filtered using a Rapid Köthen apparatus with the handsheet former equipped with a nylon sieve of 1 μm mesh size, under vacuum. The resulting wet webs are dried between two nylon sieves under vacuum at 45°C for 3 hours. The papers and nanopapers are produced after each grinding cycle (5 passes) and stored in a conditioned room at 23°C and 50% RH for 48 hours before any characterization. Low drying temperatures are selected to avoid the appearance of cracks (above 45°C) which damaged nanopapers and made it impossible to characterize them. The causes of this problem, which is not systematically observed, are not elucidated but it is certainly related to the presence of lignin.

Thickness is measured by a Lhomargy micrometer at different locations on the paper or nanopaper, and an average value is used for further calculation (m). Young's modulus of the produced materials is measured according to the NF Q03-004 standard by using a vertical extensometer (Instron 5965), with a distance between jaws of 10 cm. The width of the sample is equal to 15 mm and the tensile tests are performed at 10 mm/min. For each specimen, at least three measurements are made.

2.6 X-ray diffraction (XRD)

Papers and nanopapers samples are deposited on a zero-bottom Si substrate. X-ray diffraction (XRD) is performed by a diffractometer (X'Pert Pro MPD, PANalytical, The Netherlands) with a Bragg-Brentano geometry and a copper anode (Kα λ =1.5419 Å). The 2θ angle was between 6° and 60° with a range of 0.065°. The crystallinity index is calculated by the Segal method, according to the following equation (Segal et al., 1959):

$$\mathrm{CrI}\ (\%) = \frac{I_{002} - I_{am}}{I_{002}} \times 100 \qquad \text{Eq.2}$$

Where I_{002} is the peak intensity at 2θ = 22° and I_{am} is the peak intensity at 2θ = 16°.

2.7 Characterization of fibres and LCNF from suspensions and gels

- ***Scanning Electron Microscopy (SEM):*** SEM observations allow to witness the morphological changes after the different treatments. LCNF gels are diluted to 0.1% (w/w), dried under vacuum on a carbon adhesive and coated with a layer of Au/Pd. The analyses are performed on a Quanta 200 microscope (FEI, USA) in ETD mode, with an acceleration voltage of 10.0 kV. For each sample, at least 10 images are recorded, with magnifications between 100 and 6000.
- ***Transmission electron microscopy (TEM):*** Transmission electron microscopy (TEM) is performed on suspensions sampled in the supernatant of the LCNF gels diluated at around 0.1wt%, after 24 hours of decantation to remove micrometic fragments. TEM grids glow-discharged carbon-coated are used as support, on which droplets of the sample are deposited. Afterwards, uranyl acetate is used to negatively stain the sample. After drying, the samples are observed by a JEOL JEM-2100-Plus microscope operating at 200 kV, equipped with a Gatan Rio 16 digital camera.
- ***Morphological properties:*** NeoMorFi is a tool for characterizing the morphological properties of fibres and fine elements suspended in water. The first device has been

developed by LGP2 in partnership with the technical center of paper CTP and Techpap in France (Tourtollet et al., 2003). This analysis is based on the image processing of a very diluted suspension. To this purpose, 40 mg of dry matter are dispersed in 1 L of water, and poured in the equipment. After a second dilution, the suspension flows between two transparent plates, which allows visualizing the elements and their capture by a high resolution camera. These images are analyzed by an image processing software, leading to different parameters such as the fibre length and width, the number of fibres and fine elements, etc. The selected method defines fine elements as elements with length below 80 µm with a fixed analysis time of 5 min.

- ***Gel viscosity:*** Apparent viscosity of the gels at 2% (w/w) is measured with a DV-E viscometer (Brookfield, USA) using a disc spindle (sp-63) and a rotation speed of 50 min^{-1}.

2.8 Quality index

The quality index was developed by Desmaisons et al. (2017) to evaluate the quality of cellulose nanofibrils by including properties at different scales (macro, micro and nanometric). The calculation of this index is based on four tests applied either on the nanocellulosic suspension or the nanopapers.

$$QI^{*} = 0.3\,x_1 - 0.03\,x_2 - 0.072\,x_3^2 + 2.54\,x_3 - 5.34\,\mathrm{Ln}(x_4) + 58.62 \qquad \text{Eq.3}$$

where x_1 is the nanosized fraction (%); x_2 the turbidity (NTU); x_3 the Young's modulus (GPa) and x_4 the macro-size (μm^2) measured from optical microscopy images.

Nanosized fraction is assessed according to a protocol adapted from Naderi et al. (2015). It allows determining the amount of nanoscale particles in the suspension using a gravimetric method. LCNF gels are previously diluted to 0.02% (w/w), to be below the percolation threshold concentration, and then centrifuged at 2500 rpm (1000 g) for 15 minutes to remove the coarse components. The concentrations of the supernatant before and after centrifugation

are measured and the nanoscale fraction of the suspension is calculated using the following equation:

$$NF(\%) = \frac{C_{ac}}{C_{bc}} * 100 \quad \text{Eq.4}$$

where C_{ac} and C_{bc} correspond to the concentration (w/w) after and before centrifugation, respectively.

Turbidity of 0.1% (w/w) LCNF suspensions is measured after a dispersion step using Ultra-Turrax for one minute. A portable turbidimeter (AL 250 T-IT), with a range between 0.01 and 1100 NTU, is used. Turbidity depends on the size, number and refractive index of the visible suspended particles.Theoretically, the presence of nanoparticles in a suspension leads to a very low turbidity value. A minimum of 5 measurements are done and averages are calculated.

In order to determine the average size of microparticles, containing-lignin cellulose nanoofibrils suspensions, dispersed at 0.5% (w/w) with an Ultra-Turrax for 1 minute, are observed using optical microscopy. An optical microscope (Carl Zeiss Axio Imager M1) equipped with an AxioCam MRc 5 is used to take pictures at 5X magnification.The images are converted to 8-byte and thresholded (Fijii software). The particles analysis is the total area divided by the number of particles counted. At least, five pictures are taken and the most representative ones are used.

3. Results and discussion

3.1 Pulp characterization before mechanical pretreatment

Regarding fibre extraction, carried out in alkaline conditions, the conventional treatment (A), performed in electrically-heated rotating autoclaves is compared to the steam explosion (SE). Unbleached fibres of *Posidonia oceanica* balls (U-POB), extracted by the two different processes (autoclave: U-POB-A and steam explosion: U-POB-SE), were analysed. SEM

355 images (Figure 2, panel A) show that the extracted fibres appear to be individualised, with
356 little damage, a smooth surface and spiral shape. In our case, the imaging technique does not
357 allow to see any differences between the two pulps.

358 **Table 1.** Fibre properties after alkali-treatment.

Sample names	U-POB-A	U-POB-SE
Fibre length (µm)	272 ± 2	283 ± 2
Fibre width (µm)	19.0 ± 0.1	17.0 ± 0.5
Fine content (%)	25,0 ± 0.5	20,0 ± 0.3
Water retention value (%)	129 ± 1	101 ± 9

359

360 Morphological analyses carried out by NeoMorfi (Table 1) show that the exploded pulp, U-
361 POB-SE, has longer fibres compared to autoclave fibres, and contains more fine elements.
362 The fibre width values are quite close (17 and 19 µm). Furthermore, U-POB-A presents a
363 higher water retention value (WRV) than U-POB-SE. This reflects the swelling capacity of
364 fibres. In fact, WRV depends on the number of sites that allow hydrogen bonding with water
365 and it is favoured by a low content in lignin and a high content in hemicelluloses and
366 potentially amplified by the presence of fine elements. Klason lignin contents reported in
367 Table 2, confirm a lower lignin content for autoclave fibres (U-POB-A) than exploded fibres
368 (U-POB-SE). For the two pulps (*Posidonia* fibres extracted in autoclave or by steam
369 explosion, in alkaline conditions), there is no significant difference in hemicellulose content
370 which is ranging between 8 and 10%.

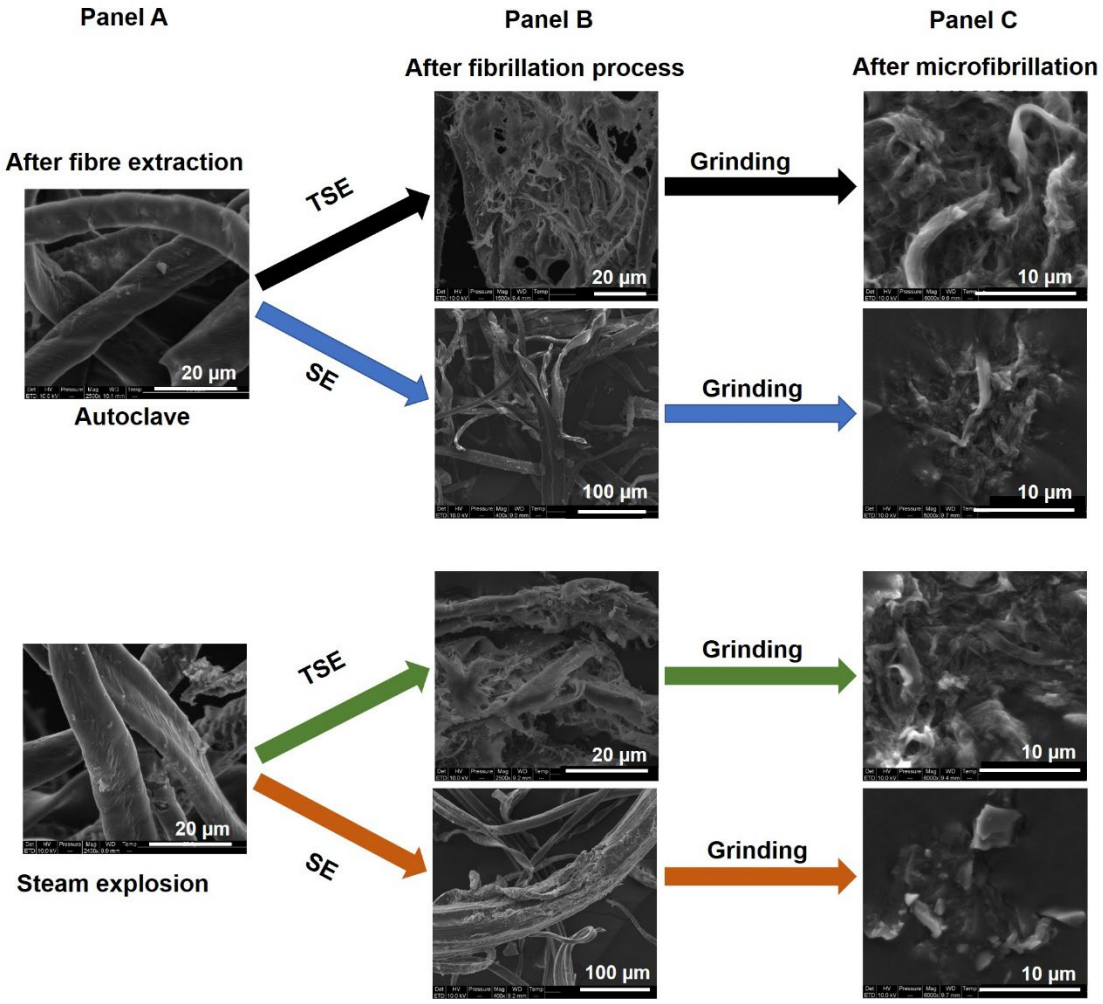

371

372 **Figure 2.** SEM observations after fibre extraction (panel A), fibrillation process (panel B) and
373 microfibrillation process (panel C).

374 To summarize, the steam exploded pulp is characterized by a slightly higher content in lignin,
375 a lower WRV, longer fibres and a lower amount of fine elements. These results reflect a less
376 intense treatment during the steam explosion compared to the autoclave pulping. This is due
377 to the lower percentage of soda (10% (w/w) for steam explosion vs. 20% (w/w) for autoclave)
378 and experimental conditions (temperature/pressure and time). The reaction yields are in line
379 with these results (around 60% and 70% after autoclave and steam explosion treatment,
380 respectively). Finally, it should be mentioned that paper preparation from these two pulps was
381 hardly feasible. In case it is successful, it was not possible to characterize them by tensile test,
382 for instance, because of their weakness. Their refining in PFI mill was also quite impossible

due to a very poor pulp quality and a low strength of the wet mat. This particular behaviour of *Posidonia* fibres was already observed in a previous study (Khiari, 2010).

Table 2. Lignin content, crystallinity index and mechanical properties of papers before and after pretreatments.

Sample names	Lignin content (%)	CrI (%)	Paper density (kg/ m^{-3})	Paper Young's modulus (GPa)
U-POB-A	29	n.m	n.d	n.d
U-POB-A-TSE	26	42	587	1.5
U-POB-A-SE	24	41	377	0.4
U-POB-SE	34	n.m	328	0.1
U-POB-SE-TSE	32	40	458	0.6
U-POB-SE-SE	14	35	316	0.1

3.2 Pulp characterization after pretreatments

To overcome the difficulties related to refining, extracted fibres (U-POB-A and U-POB-SE) were pre-treated using either twin-screw extrusion (1 pass) or steam explosion (3 times). Extrusion or steam explosion were thus applied instead of a conventional refining. Lignin content, morphological, physical and mechanical properties were then analysed after the pretreatments.

Figure 3 shows that, for U-POB-A-TSE, twin-screw extrusion interestingly reduced fibre length from 272 µm to 148 µm, as steam explosion did it but in a less extent (from 272 µm to 220 µm).

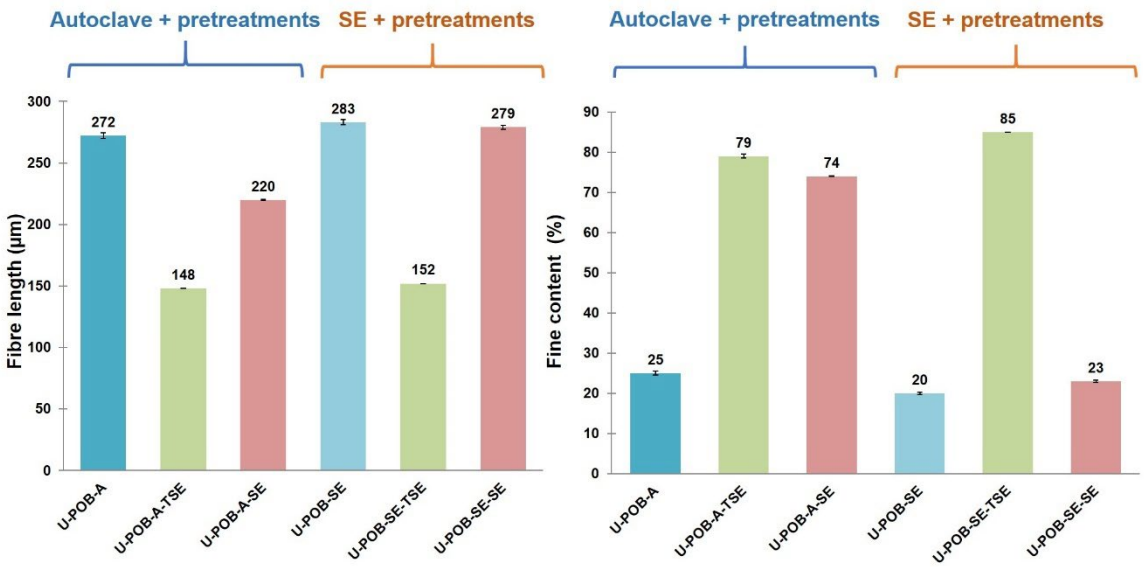

Figure 3. Morphological properties after pretreatments.

NeoMorFi revealed quite similar fine contents of the extruded pulps, varying between 74% and 85% for U-POB-SE-TSE and U-POB-A-TSE, respectively. It is important to highlight that the thrice-exploded pulp U-POB-SE-SE shows a very low fine content. This result, which was not expected, is due to a poorly adapted filtration method after steam explosion (nylon sieve of 40 µm mesh size). Trials were carried out by using a nylon sieve of 1 µm mesh size and a rate of lost fines of 10% was obtained. Unfortunately, filtration with a reduced mesh size was time-consuming which did not allow its use. So, when the filtration step after steam explosion is done three times, a significant part of the fines are lost during the washing step. This problem must be kept in mind as it will be affect the obtained results. The SEM images (Figure 2, panel B) show that twin-screw extrusion induces large changes in the fibre morphology and a partial detachment of the macrofibrils (for both kind of extracted fibers). This phenomenon is less visible in the case of steam explosion applied as a fibrillation process, resulting in a lower degree of refining visually.

Papers are prepared and characterized by determining their density, Young's modulus and crystallinity index. Indeed, the density reflects the effect of the pretreatment. This property is closely related to the external fibrillation and aspect ratio of the fibres, and their flexibility,

415 which depends on their hydration (internal fibrillation). Fine elements also play an important
416 role in clogging the network and making the paper denser (Afra et al., 2013). According to the
417 values reported in Table 2, twin-screw extrusion combined with an autoclave pulping U-POB-
418 A-TSE produces the densest paper with the highest Young's modulus. On the other hand,
419 thrice exploded pulp U-POB-SE-SE exhibits the lowest density and the lowest Young's
420 modulus (316 kg m^{-3} and 0.1 GPa). It is important to recall that the loss of fine elements
421 during filtration method may be the main reason. Whatever the considered pretreatment, it
422 appears that the obtained paper have low density and Young's modulus. This is consistent
423 with the poor strength of the paper before the pretreatments. Despite this observation, twin-
424 screw extrusion as well as steam explosion, even if the effect is less pronounced for the latter,
425 are able to improve the properties of the prepared papers.
426 Concerning the crystallinity index (see Table 2), it is close to 40% for U-POB-SE-TSE , U-
427 POB-A-SE and U-POB-SE-TSE but it is lower for U-POB-SE-SE (around 35%). Indeed, the
428 severe and successive applied steam explosions may degrade the cellulosic fibres. As
429 expected, Klason lignin (see Table 2) was found to be lower for the three-time exploded pulp;
430 even if the time residence was reduced, delignification still occurred in these conditions. As
431 expected, the hemicellulose content remains unchanged after the different mechanical
432 pretreatments.

433 **3.3 LCNF properties**

434 The obtained pulps, after extrusion or steam explosion, were ground under same conditions.
435 The effect of the combined treatments on the quality of LCNF (viscosity and morphological
436 properties of the gels, mechanical properties of the nanopapers and quality index) and on the
437 energy consumed by the grinding process was then evaluated. To this purpose, the
438 suspensions/gels and the obtained nanopapers were characterized at different stages during
439 grinding.

3.3.1. Morphology

Figure 4.1 shows optical microscopy images of the gels after TSE or SE and grinding. Neither the combination of SE, nor TSE with grinding totally eliminated residual fibres in the obtained gels: in all cases, residual fibres were still present. Non-fibrillated fibre fragments were also observed, indicating a relatively low degree of microfibrillation. However, these processes have a strong impact on the fibre morphology. NeoMorFi analyzer, allowing a more quantitative analysis, show that fine content varies between 96 and 99% for all the samples. As expected, after grinding, the number of residual fibres was slightly lower and their length was reduced to be in the range between 113 and 120 μm. Comparing gels, fibre content was higher for U-POB-SE-SE-M reaching 40 millions, while for U-POB-A-TSE-M, fibre content was the lowest to be 5 millions. This highlights the efficiency of the twin-screw extruder as a pretreatment. It is an important to note that the low resolution of the optical microscope and NeoMorFi did not allow the detection of finer elements. So, even if same morphologies were observed for all the ground samples it does not mean that microfibrillation is equivalent.

Figure 2 (panel C) shows SEM images of the produced LCNF after the ultra-fine friction grinder. Thes images illustrate obivously the presence of partially individualised microfibril bundles. It is important to mention, due to the resolution of the SEM, that the actual structure of the cellulose microfibrils bundles cannot be clearly revealed. U-POB-A-TSE-M, U-POB-A-SE-M and U-POB-SE-TSE-M present similar scanning electron micrographs. The combination of mechanical processes leads to the production of a high proportion of non-nanofibrillated and/or macro/microfibres, as indicated by their low microfibrillation yield (see Table 4). U-POB-SE-SE-M aspect is quite different, no fibril networks beign observed. Generally, all suspensions with a fairly high residual lignin content contained more fibrous, partially fibrillated structures and fibril bundles (Lahtinen et al., 2014; Yuan et al., 2021).

Table 3. Estimation of elements size.

	Microfibrillar bundles (nm)	Microfibrils (nm)	Elementary fibrils (nm)
U-POB-A-TSE-M	230	38	9
U-POB-SE-TSE-M	348	39	8
U-POB-A-SE-M	354	40	9
U-POB-SE-SE-M	170	62	8

Transmission electron microscopy (TEM) images also show partially desctructered microfibrillated bundles, with more individualized and finer microfibrils at their ends (Figure 4.2). In all samples, different units of the hierarchical structure of the fibres are present: microfibrillar bundles with a width of a few hundred nanometers (from 170 to 350 nm), microfibrils with a width of a few dozen nanometers (from 40 to 60 nm) and some nanofibrils with a width of a few nanometers (around 9 nm), see Table 3. The size distribution of the elements is thus large, indicating that microfibrillation is partial. However, the obtained bundles are very damaged.

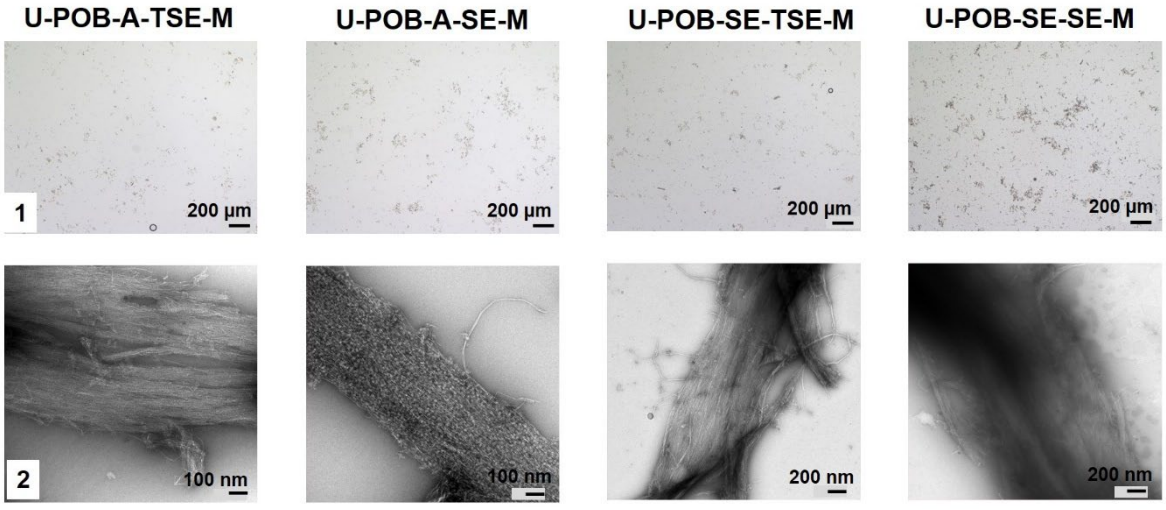

Figure 4. Microscopic observations, (1) optical, (2) TEM.

3.3.2. Viscosity

During grindind, pulps passing through the gap between the stone discs is subjected to compression and shear forces. It is believed that the shear forces become a dominant factor in mechanical processing as the gap decreases. Grinding action promotes the generation of fines, by peeling-off of the outer surface of the fibres (Kang and Paulapuro, 2006). In fact, the specific energy measured by power monitoring during grinding increases with time and with the change in the gap between the discs and the disc rotation speed (Figure 5.1). In this context, Kang and Paulapuro (2006) reported that the specific energy of the ultra-fine grinding increases as the disc gap decreases, in the same line as the development of internal fibrillation and external fibrillation. Moreover, the rheological properties of gels were measured using a spindle based on paddle geometry. This method is accepted as a practical way to test a polydispersed viscous system. Actually, this method is particularly advantageous for heterogeneous materials such as microfibrillated cellulose (Lahtinen et al., 2014). In general, the increase in viscosity of a fibrous suspension during microfibrillation is due to the formation of a solid network of entangled microfibres (Pääkkö et al., 2007).

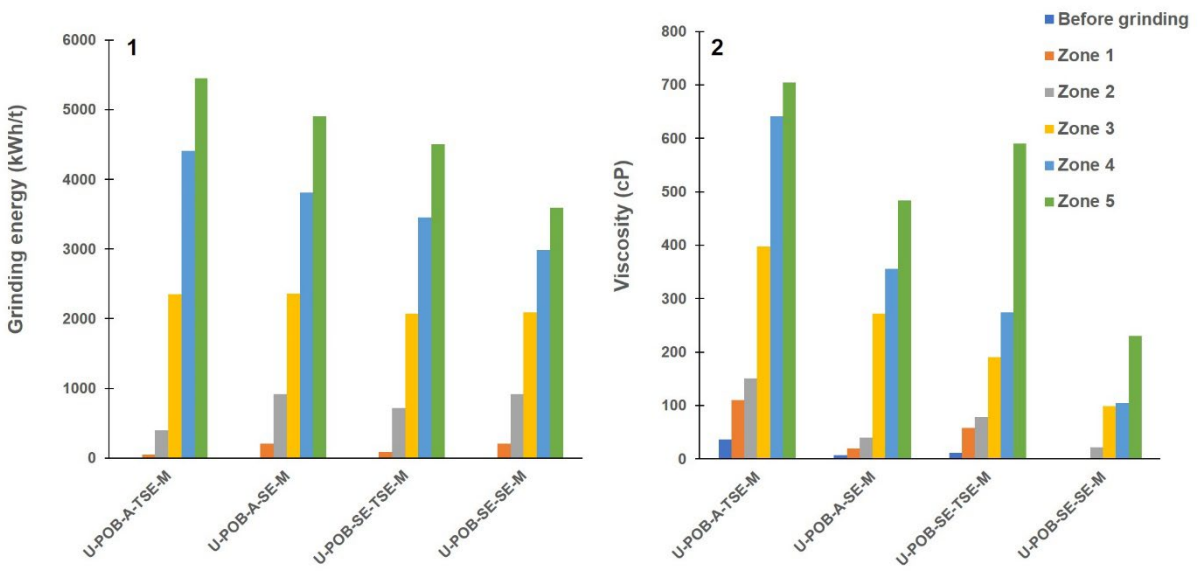

Figure 5. Energy consumption during grinding (1) and Viscosity values (2). Zone 1: 5 passes at 0 (contact mode) between 950 and 1200 rpm, Zone 2: (1) + 5 passes at the gap -5 between 1200 and 1500 rpm, Zone 3: (2) + 5 passes at the gap -10 at 1500 rpm, Zone 4: (3) + 5 passes at the gap -10 at 1500 rpm, Zone 5: (4) + 5 passes at the gap -10 at 1500 rpm.

The evolution of the suspension viscosity before and after ultra-fine grinding is shown in Figure 5.2. It increases as a function of zones/cycles, grinding time, and grinding energy. U-POB-A-TSE-M (alkaline pulping in autoclave) reached the highest viscosity value (705 cP), while the viscosity for U-POB-SE-TSE-M (alkaline pulping by steam explosion) present a value of 590 cP. This proves, once again, the effectiveness of TSE as a pretreatment whatever the used method for pulping. For U-POB-A-SE-M and U-POB-SE-SE-M (where steam explosion process was used as a pretreatment), viscosity values were between 484 and 230 cP, respectively. These low values can be associated to the presence of a non-negligible percentage of residual fibres or microfibrils bundles. These elements, with a low aspect ratio, are less entangled, which leads to the formation of a weaker microfibres network. As the viscosity of samples pre-treated by steam explosion is significantly lower than those extruded, it can be concluded that (SE) does not lead to an efficient pulp microfibrillation. A possible explanation is the chopping of fibres into smaller elements instead of fibrillating them, which conducts to the production of a heterogeneous material with elements of low aspect ratio.

514 It appears that the samples (apart from U-POB-A-TSE-M) did not reach their maximum
515 viscosities after twenty-five passes through the ultra-fine friction grinder (Figure 6),
516 suggesting that further grinding could still improve their properties. The energy consumption
517 for U-POB-A-TSE-M was around 5400 kWh/t, which was the highest compared to the other
518 samples. Among the produced suspensions, U-POB-SE-TSE-M had the lowest energy
519 consumption, around 3600 kWh/t.

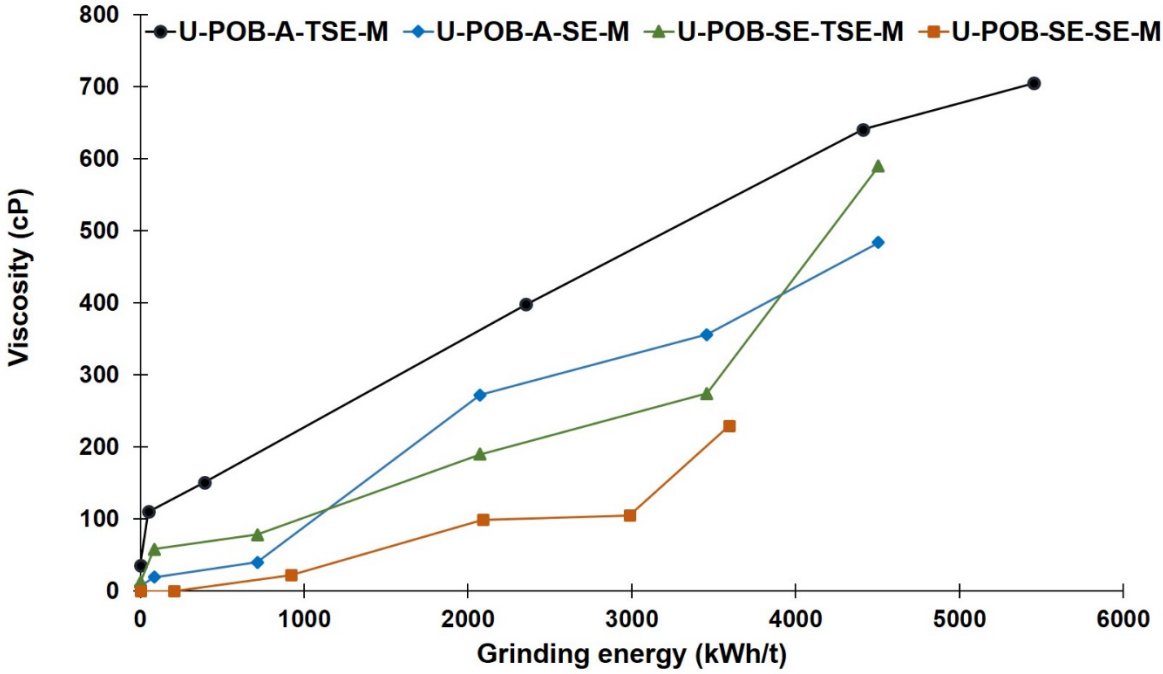

520

521 **Figure 6**. The evolution of gel viscosity as function of energy.

522 ***3.3.3. Physical and mechanical properties***

523 Figure 7 shows how Young's modulus of papers and nanopapers evolves with the grinding
524 energy. As expected, before grinding, papers have low tensile properties. During grinding,
525 microfibrils are more and more released and bonding degree of the nanopapers increases, with
526 a direct impact on their physical properties (Cuberos-Martinez and Park, 2012; Henriksson et
527 al., 2008; Nair et al., 2014; Stelte and Sanadi, 2009). Nanopapers thus show a higher density,
528 which approximately varies from 300 to 1200 kg.m^{-3}, and an improvement of the resistance to
529 deformation illustrated by the increase of the Young's modulus (see Figure 7.2).

When twin-screw extrusion is used as pretreatment for both alkali pulping in autoclave and steam explosion reactor (U-POB-A-TSE-M and U-POB-SE-TSE-M), the obtained nanopapers present the highest Young's modulus, around 6 and 4 GPa, respectively. When steam explosion is used as pretreatment for alkali pulping in autoclave and steam explosion reactor (U-POB-A-SE-M and U-POB-SE-SE-M), lower elastic modulus of 4 and 2 GPa, respectively, are measured.

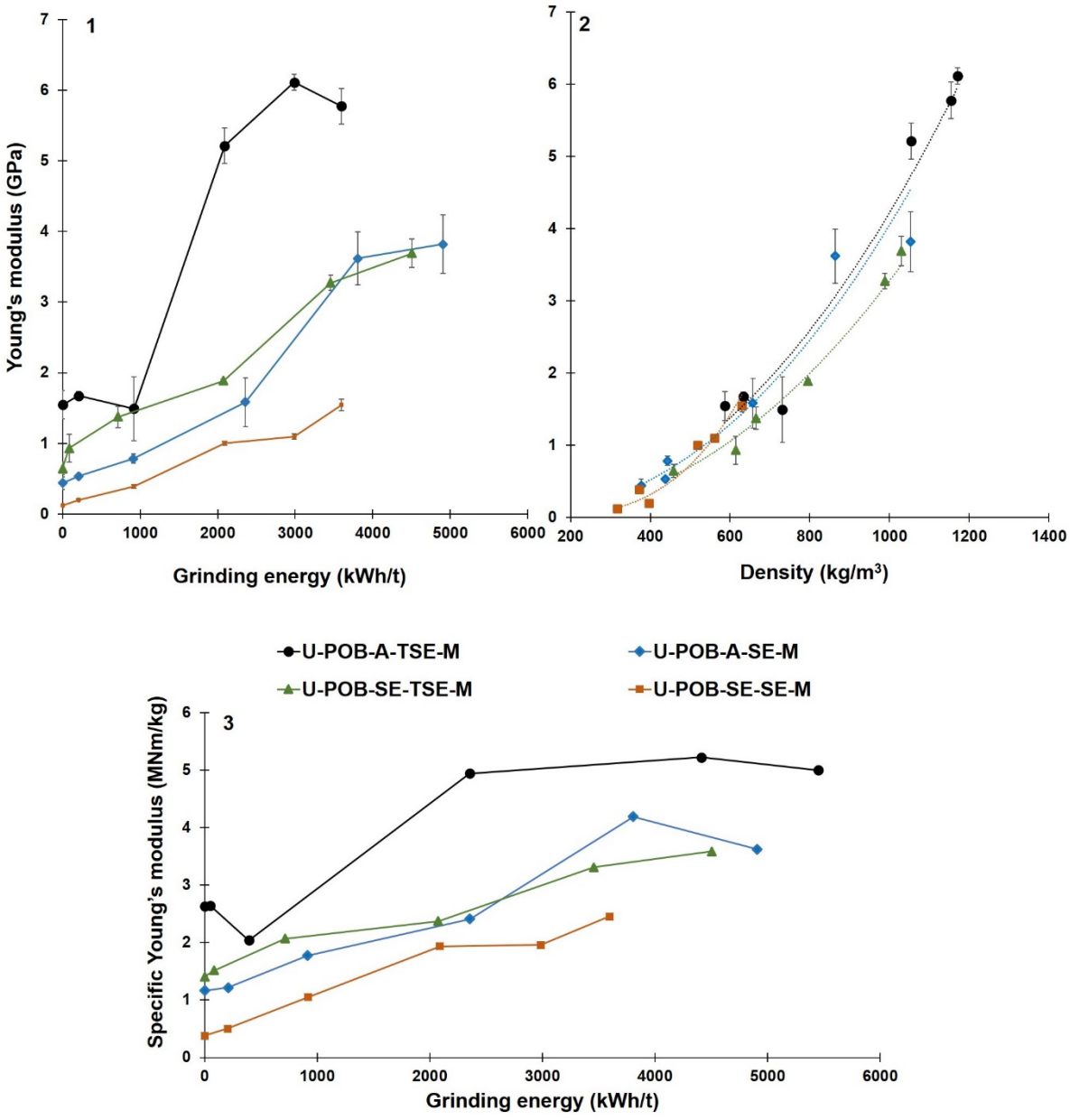

Figure 7. Evolution of Young's modulus as a function of grinding energy (7.1), as a function of density (7.2) and the evolution of specific Young's modulus as a function of grinding energy (7.3).

Figure 7.3 reports the variation of the specific Young's modulus with grinding energy. It is worth noting that these values significantly evolve at the beginning of the grinding process with increases above 100 %. In contrast, they remain more or less constant or change less importantly when grinding energy increases. This could be attributed to a drastic modification of the porous structure of the samples, when passing from papers to nanopapers, this phenomenon occuring for grinding energy less than 2000-3000 kWh/t. Then, even if the bonding degree continues increasing, as it is shown by the increase in density of the nanopapers, their structure does not change to the same extent and the specific Young's modulus even seems to reach a plateau value for certain samples.

3.3.4. Simplified quality index

After grinding, and for extruded pulps, nanosized fraction was around 56% whatever the pulping process used (Table 4). In contrast, when steam explosion is used as the main mechanical pretreatment process, nanosized fraction is lower and the values depends on the pulping process: nanosized fraction is equal to 50% for autoclave pulping and 32% for steam explosion pulping (Table 4). These results again prove that TSE is by far more efficient when it is used as a mechanical pretreatment before grinding than steam explosion. Indeed, due to its fibrillation capacity, TSE is able to replace, at least partially, a conventional refining step: in the tested operating conditions, this is not the case of the steam explosion process, even it it was thrice done.

For all the obtained gels, turbidity and macro-scale fraction measurements were not able to differentiate samples. The large size distribution of the elements present in the gels leads to similar and high values of turbidity (≈ 930 NTU, calculated as an average of all the values). In the same way, the micro-scaled size ranges between 12 and 19 μm^2 for all the samples.

As discussed in the previous section, steam explosion procedure leads to an important loss in fine elements, particularly when this process is repeated three times. This phenomenon can explain the very low Young's modulus measured for the corresponding nanopapers (about 2 GPa). Thus, when SE is used as a pretreatment, its effects are probably underestimated in this work due to the above mentioned reason.

The quality index QI* of *Posidonia*-LCNF produced from extruded pulps ranges from 45 to 48, depending on the pulping process. As expected, the values are lower when SE is used (see Table 4). Nader et al. (2022) reported a quality index between 52 and 57 for LCNF obtained from wood (*Eucalyptus Globulus* barks), refined and ground by ultra-fine friction grinder , after autoclave and SE pulping in alkaline conditions. Espinosa et al. (2020) and Taha et al. (2021) produced LCNF from wheat and rice straw with a quality index of 77 and 81, respectively (see Table 4). These higher values can be explained by more severe conditions of grinding as well as the higher quality of the raw material. Nevertheless, it is worth noting that the quality index was initially proposed for CNF produced from bleached and pretreated fibres (enzymatic or chemical pretreatment). Its use for LCNF gels should be considered with caution and comparison with quality index of conventional CNF is uncertain.

Table 4. Quality indexes for LCNF obtained in this work and comparison with the literature.

Samples	Average micro particle size (μm^2)	Nanosized fraction (%)	Turbidity (NTU)	Young's modulus (GPa)	QI*
U-POB-A-TSE-M	15.2 ± 5.9	56.3 ± 3.4	907	5.8 ± 0.0	48.4 ± 2.9
U-POB-A-SE-M	19.0 ± 7.0	49.7 ± 0.9	907	3.8 ± 0.4	41.5 ± 2.8
U-POB-SE-TSE-M	12.8 ± 6.2	56.3 ± 3.4	907	3.7 ± 0.2	45.5 ± 3.5
U-POB-SE-SE-M	15.7 ± 4.0	31.8 ± 2.1	907	1.5 ± 0.1	31.9 ± 1.5
Rice straw pulp Taha et al. (2021)*	n.m	78.9 ± 3.9	404 ± 9.6	6.3 ± 0.2	81 ± 12
Wheat straw pulp Espinosa et al. (2020)**	19.4 ± 2.5	62.5 ± 6.3	245 ± 6.3	16.7 ± 0.7	76.5 ± 1.1

n.m: non-mentioned; * Taha et al. (2021): Production of LCNF (14% of lignin content) from rice straw, refined by Valley beater and ground by ultra-fine friction grinder.;**Espinosa et al. (2020): Production of LCNF (9% of lignin content) from wheat straw pulp, refined by PFI mill and ground by ultra-fine friction grinder.

Finally, an attempt was made to monitor the quality index as a function of the energy consumed during grinding. Figure 8 exhibits important differences between the samples. Both methods (A-SE-M and SE-SE-M) produced gels with less energy consumption but lower quality. The use of steam explosion as a pretreatment before ultra-fine friction grinder does not bring much more in terms of fibrillation, but, for the moment, it is not possible to assert whether this is a limitation of the process or a defect in the adaptation of the filtration method.

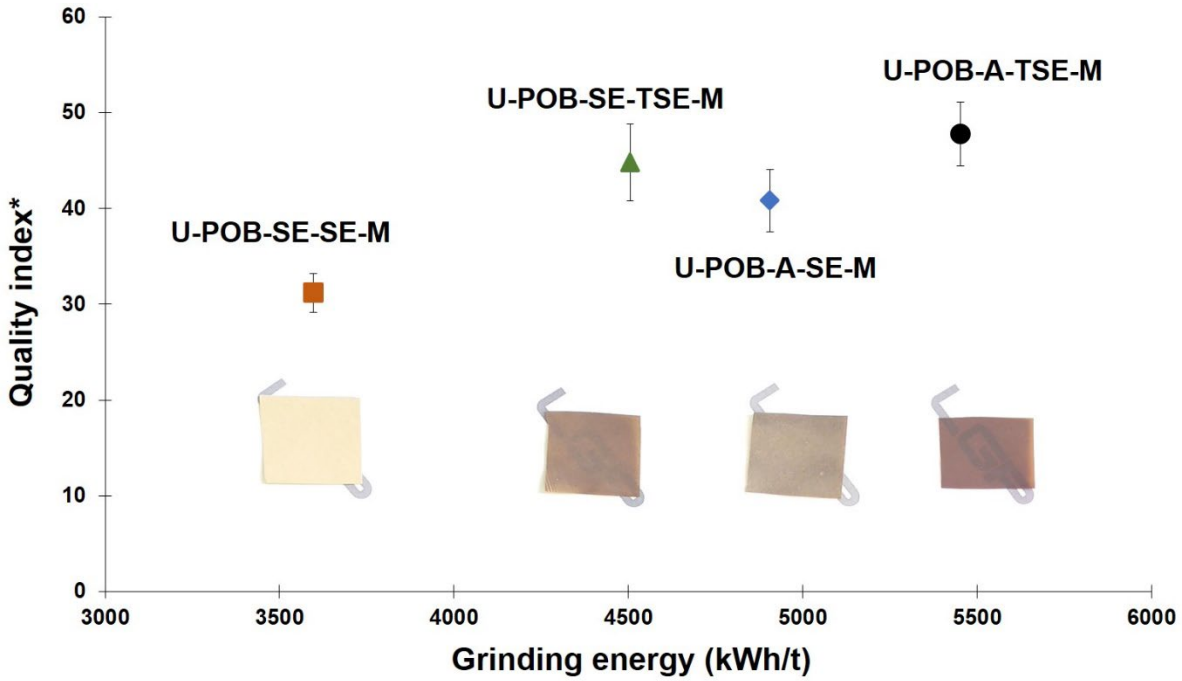

Figure 8. Evolution of quality index in fuction of grinding energy.

4. Conclusion

The aim of this study is to propose a solution allowing to treat the non-delignified material resulting from non-conventional biomass from marine waste: *Posidonia oceanica*. The production of lignin-containing cellulose nanofibrils from *Posidonia* was achieved from two different extraction methods using conventional autoclave and steam explosion. The

advantage of the proposed combinations is the elimination of bleaching and chemical pretreatment step. It was found that steam explosion could be used for fibre extraction as an alternative of autoclave but its use for a mechanical pretreatment replacing refining should be optimized to avoid the loss in fine elements. Furthermore, twin-screw extrusion showed its ability to promote internal and external fibrillation and replace refining for this raw material. Finally, LCNF production, with an acceptable quality (45 to 50%), was possible by the combination of steam explosion or autoclave for fibre extraction, twin-screw extrusion and grinding. These product could be used in different applications, which do not require a high quality of nanomaterials, such as board/papermaking and bionanocomposite. To open new perspectives, it could be interesting to apply these procedures to a more conventional raw material. Another interesting approach would be in relation to the decrease in a greater extent the lignin content. Considering all these aspects, the efficiency of the proposed combination of processes is then probably underestimated.

Acknowledgements

This work was financially supported by the "PHC Utique" program of the French Ministry of Foreign Affairs and Ministry of higher education, research and innovation and the Tunisian Ministry of higher education and scientific research in the CMCU project number TN 18G1132// FR 39316VF. LGP2 is part of the LabEx Tec 21 (Investissements d'Avenir - grant agreement n°ANR-11-LABX-0030) and of PolyNat Carnot Institute (Investissements d'Avenir - grant agreement n° ANR-16-CARN-0025-01). This research was made possible thanks to the facilities of the TekLiCell platform funded by the Région Rhône-Alpes (ERDF: European regional development fund). In addition, the authors would like to thank Thierry Encinas from CMTC – Grenoble, France for the XRD analysis, and Jean-Luc Puteaux from CERMAV Grenoble, France for TEM observations.

References

Ago, M., Ferrer, A., Rojas, O.J., 2016. Starch-Based Biofoams Reinforced with Lignocellulose Nanofibrils from Residual Palm Empty Fruit Bunches: Water Sorption and Mechanical Strength. ACS Sustainable Chem. Eng. 4, 5546–5552. https://doi.org/10.1021/acssuschemeng.6b01279

Ämmälä, A., Laitinen, O., Sirviö, J.A., Liimatainen, H., 2019. Key role of mild sulfonation of pine sawdust in the production of lignin containing microfibrillated cellulose by ultrafine wet grinding. Industrial Crops and Products 140, 111664. https://doi.org/10.1016/j.indcrop.2019.111664

Avella, R., Scoditti, E., 1998. The Italian steam explosion program at ENEA. Biomass and Bioenergy 14, 289–293. https://doi.org/10.1016/S0961-9534(97)10041-1

Benito-González, I., López-Rubio, A., Gavara, R., Martínez-Sanz, M., 2019. Cellulose nanocrystal-based films produced by more sustainable extraction protocols from Posidonia oceanica waste biomass. Cellulose 26, 8007–8024. https://doi.org/10.1007/s10570-019-02641-4

Bettaieb, F., Khiari, R., Dufresne, A., Mhenni, M.F., Putaux, J.L., Boufi, S., 2015. Nanofibrillar cellulose from Posidonia oceanica: Properties and morphological features. Industrial Crops and Products 72, 97–106. https://doi.org/10.1016/j.indcrop.2014.12.060

Boonterm, M., Sunyadeth, S., Dedpakdee, S., Athichalinthorn, P., Patcharaphun, S., Mungkung, R., Techapiesancharoenkij, R., 2016. Characterization and comparison of cellulose fiber extraction from rice straw by chemical treatment and thermal steam explosion. Journal of Cleaner Production, Special Volume: Green and Sustainable Innovation for Cleaner Production in the Asia-Pacific Region 134, 592–599. https://doi.org/10.1016/j.jclepro.2015.09.084

Chen, X., Zhang, Y., Gu, Y., Liu, Z., Shen, Z., Chu, H., Zhou, X., 2014. Enhancing methane production from rice straw by extrusion pretreatment. Applied Energy 122, 34–41. https://doi.org/10.1016/j.apenergy.2014.01.076

Chinga-Carrasco, G., Ehman, N.V., Pettersson, J., Vallejos, M.E., Brodin, M.W., Felissia, F.E., Håkansson, J., Area, M.C., 2018. Pulping and Pretreatment Affect the Characteristics of Bagasse Inks for Three-dimensional Printing. ACS Sustainable Chem. Eng. 6, 4068–4075. https://doi.org/10.1021/acssuschemeng.7b04440

Cuberos-Martinez, P., Park, S.W., 2012. REVIEW OF PHYSICAL PRINCIPLES IN LOW CONSISTENCY REFINING 73, 8.

Deepa, B., Abraham, E., Cherian, B.M., Bismarck, A., Bismarck, A., Blaker, J.J., Pothan, L.A., Leao, A.L., Souza, S.F., Kottaisamy, M., 2011. Structure, morphology and thermal characteristics of banana nano fibers obtained by steam explosion. Bioresour. Technol 1988–1997.

Delgado-Aguilar, M., González, I., Tarrés, Q., Pèlach, M.À., Alcalà, M., Mutjé, P., 2016. The key role of lignin in the production of low-cost lignocellulosic nanofibres for papermaking applications. Industrial Crops and Products 86, 295–300. https://doi.org/10.1016/j.indcrop.2016.04.010

Desmaisons, J., Boutonnet, E., Rueff, M., et al, 2017. A new quality index for benchmarking of different cellulose nanofibrils. Carbohydr Polym 318–329.

Diop, C.I.K., Lavoie, J.-M., Huneault, M.A., 2015. Structural changes of Salix miyabeana cellulose fibres during dilute-acid steam explosion: Impact of reaction temperature and retention time. Carbohydrate Polymers 119, 8–17. https://doi.org/10.1016/j.carbpol.2014.11.031

669 Duque, A., Manzanares, P., Ballesteros, M., 2017. Extrusion as a pretreatment for
670 lignocellulosic biomass: Fundamentals and applications. Renewable Energy 114,
671 1427–1441. https://doi.org/10.1016/j.renene.2017.06.050
672 Ehman, N.V., Lourenço, A.F., McDonagh, B.H., Vallejos, M.E., Felissia, F.E., Ferreira,
673 P.J.T., Chinga-Carrasco, G., Area, M.C., 2020. Influence of initial chemical
674 composition and characteristics of pulps on the production and properties of
675 lignocellulosic nanofibers. International Journal of Biological Macromolecules 143,
676 453–461. https://doi.org/10.1016/j.ijbiomac.2019.10.165
677 Espinosa, E., Rol, F., Bras, J., Rodríguez, A., 2020. Use of multi-factorial analysis to
678 determine the quality of cellulose nanofibers: effect of nanofibrillation treatment and
679 residual lignin content. Cellulose. https://doi.org/10.1007/s10570-020-03136-3
680 Espinosa, E., Tarrés, Q., Delgado-Aguilar, M., González, I., Mutjé, P., Rodríguez, A., 2016.
681 Suitability of wheat straw semichemical pulp for the fabrication of lignocellulosic
682 nanofibres and their application to papermaking slurries. Cellulose 23, 837–852.
683 https://doi.org/10.1007/s10570-015-0807-8
684 Ewulonu, C.M., Liu, X., Wu, M., Huang, Y., 2019. Ultrasound-assisted mild sulphuric acid
685 ball milling preparation of lignocellulose nanofibers (LCNFs) from sunflower stalks
686 (SFS). Cellulose 26, 4371–4389. https://doi.org/10.1007/s10570-019-02382-4
687 Ferrer, A., Hoeger, I.C., Lu, X., Rojas, O.J., 2016. Reinforcement of polypropylene with
688 lignocellulose nanofibrils and compatibilization with biobased polymers. Journal of
689 Applied Polymer Science 133. https://doi.org/10.1002/app.43854
690 Ferrer, A., Quintana, E., Filpponen, I., Solala, I., Vidal, T., Rodríguez, A., Laine, J., Rojas,
691 O.J., 2012. Effect of residual lignin and heteropolysaccharides in nanofibrillar
692 cellulose and nanopaper from wood fibers. Cellulose 19, 2179–2193.
693 https://doi.org/10.1007/s10570-012-9788-z
694 Fortunati, E., Luzi, F., Puglia, D., Petrucci, R., Kenny, J.M., Torre, L., 2015. Processing of
695 PLA nanocomposites with cellulose nanocrystals extracted from Posidonia oceanica
696 waste: Innovative reuse of coastal plant. Industrial Crops and Products 67, 439–447.
697 https://doi.org/10.1016/j.indcrop.2015.01.075
698 Hanhikoski, S., Solala, I., Lahtinen, P., Niemelä, K., Vuorinen, T., 2016. Lignocellulosic
699 nanofibrils from neutral sulphite pulps.
700 Henriksson, M., Berglund, L.A., Isaksson, P., Lindström, T., Nishino, T., 2008. Cellulose
701 Nanopaper Structures of High Toughness. Biomacromolecules 9, 1579–1585.
702 https://doi.org/10.1021/bm800038n
703 Herrera, M., Thitiwutthisakul, K., Yang, X., Rujitanaroj, P., Rojas, R., Berglund, L., 2018.
704 Preparation and evaluation of high-lignin content cellulose nanofibrils from
705 eucalyptus pulp. Cellulose 25, 3121–3133. https://doi.org/10.1007/s10570-018-1764-9
706 Hietala, M., Niinimäki, J., Oksman, K., 2011. THE USE OF TWIN-SCREW EXTRUSION
707 IN PROCESSING OF WOOD: THE EFFECT OF PROCESSING PARAMETERS
708 AND PRETREATMENT 11.
709 Holtzapple, M.T., Humphrey, A.E., Taylor, J.D., 1989. Energy requirements for the size
710 reduction of poplar and aspen wood. Biotechnology and Bioengineering 33, 207–210.
711 https://doi.org/10.1002/bit.260330210
712 Horseman, T., Tajvidi, M., Diop, C.I.K., Gardner, D.J., 2017. Preparation and property
713 assessment of neat lignocellulose nanofibrils (LCNF) and their composite films.
714 Cellulose 24, 2455–2468. https://doi.org/10.1007/s10570-017-1266-1
715 Kang, T., Paulapuro, H., 2006. New mechanical treatment for chemical pulp. Proceedings of
716 the Institution of Mechanical Engineers, Part E: Journal of Process Mechanical
717 Engineering 220, 161–166. https://doi.org/10.1243/09544089JPME81

718 Khadraoui, M., Khiari, R., Brosse, N., Bergaoui, L,. Mauret, E., 2022. Combination of steam
719 explosion and TEMPO-mediated oxidation as pretreatments to produce nanofibrils of
720 cellulose from Posidonia oceanica bleached fibres. BioResources 17(2), 2933-2958.
721 DOI: 10.15376/biores.17.2.2933-2958
722 Khiari, R., 2010. Valorisation des déchets d'origine agricole et marine : application dans les
723 domaines textiles, papetiers et des composites (phdthesis). Université Grenoble Alpes.
724 Khiari, R., Mhenni, M. F., Belgacem, M. N., Mauret, E. 2010. Chemical composition and
725 pulping of date palm rachis and Posidonia oceanica – A comparison with other wood
726 and non-wood fibre sources. Bioresource Technology, *101*(2), 775–780.
727 https://doi.org/10.1016/j.biortech.2009.08.079
728 Khiari, R., Mauret, E., Belgacem, M. N., Mhemmi, F. 2011. Tunisian date palm rachis used as
729 an alternative source of fibres for papermaking applications Palm rachis fibers for
730 paper. BioResources, 6, 265–281.
731 Lahtinen, P., Liukkonen, S., Pere, J., Sneck, A., Kangas, H., 2014. A Comparative Study of
732 Fibrillated Fibers from Different Mechanical and Chemical Pulps. BioResources 9,
733 2115–2127.
734 Leu, S.-Y., Zhu, J.Y., 2013. Substrate-Related Factors Affecting Enzymatic Saccharification
735 of Lignocelluloses: Our Recent Understanding. Bioenerg. Res. 6, 405–415.
736 https://doi.org/10.1007/s12155-012-9276-1
737 Lu, H., Zhang, L., Liu, C., He, Z., Zhou, X., Ni, Y., 2018. A novel method to prepare
738 lignocellulose nanofibrils directly from bamboo chips. Cellulose 25, 7043–7051.
739 https://doi.org/10.1007/s10570-018-2067-x
740 Luo, H., Zhang, H., Yue, L., Pizzi, A., Lu, X., 2018. Effects of steam explosion on the
741 characteristics of windmill palm fiber and its application to fiberboard. Eur. J. Wood
742 Prod. 76, 601–609. https://doi.org/10.1007/s00107-017-1259-7
743 Nader, S., Brosse, N., Khadraoui, M., Fuentealba, C., Ziegler-Devin, I., Quilès, F., El kirat
744 chatel, S., Mauret, E., 2022. Lignocellulosic micro and nanofibrils obtained from
745 eucalyptus globulus barks: Comparative study between steam explosion and
746 conventional cooking (Submitted to be Published)
747 Naderi, A., Lindström, T., Sundström, J., 2015. Repeated homogenization, a route for
748 decreasing the energy consumption in the manufacturing process of
749 carboxymethylated nanofibrillated cellulose? Cellulose 22, 1147–1157.
750 https://doi.org/10.1007/s10570-015-0576-4
751 Nair, S.S., Zhu, J.Y., Deng, Y., Ragauskas, A.J., 2014. Characterization of cellulose
752 nanofibrillation by micro grinding. J Nanopart Res 16, 2349.
753 https://doi.org/10.1007/s11051-014-2349-7
754 Osong, S.H., Norgren, S., Engstrand, P., 2013. An approach to produce nano-ligno-cellulose
755 from mechanical pulp fine materials. Nordic Pulp & Paper Research Journal 28, 472–
756 479. https://doi.org/10.3183/npprj-2013-28-04-p472-479
757 Overend, R.P., Chornet, E., Gascoigne, J.A., Hartley, B.S., Broda, P.M.A., Senior, P.J., 1987.
758 Fractionation of lignocellulosics by steam-aqueous pretreatments. Philosophical
759 Transactions of the Royal Society of London. Series A, Mathematical and Physical
760 Sciences 321, 523–536. https://doi.org/10.1098/rsta.1987.0029
761 Pääkkö, M., Ankerfors, M., Kosonen, H., Nykänen, A., Ahola, S., Österberg, M.,
762 Ruokolainen, J., Laine, J., Larsson, P.T., Ikkala, O., Lindström, T., 2007. Enzymatic
763 Hydrolysis Combined with Mechanical Shearing and High-Pressure Homogenization
764 for Nanoscale Cellulose Fibrils and Strong Gels. Biomacromolecules 8, 1934–1941.
765 https://doi.org/10.1021/bm061215p

766 Qin, L., Chen, H., 2015. Enhancement of flavonoids extraction from fig leaf using steam
767 explosion. Industrial Crops and Products 69, 1–6.
768 https://doi.org/10.1016/j.indcrop.2015.02.007
769 Rojo, E., Peresin, M.S., Sampson, W.W., Hoeger, I.C., Vartiainen, J., Laine, J., Rojas, O.J.,
770 2015. Comprehensive elucidation of the effect of residual lignin on the physical,
771 barrier, mechanical and surface properties of nanocellulose films. Green Chem. 17,
772 1853–1866. https://doi.org/10.1039/C4GC02398F
773 Rol, F., Banvillet, G., Meyer, V., Petit-Conil, M., Bras, J., 2018. Combination of twin-screw
774 extruder and homogenizer to produce high-quality nanofibrillated cellulose with low
775 energy consumption. J Mater Sci 53, 12604–12615. https://doi.org/10.1007/s10853-
776 018-2414-1
777 Rol, F., Karakashov, B., Nechyporchuk, O., Terrien, M., Meyer, V., Dufresne, A., Belgacem,
778 M.N., Bras, J., 2017. Pilot-Scale Twin Screw Extrusion and Chemical Pretreatment as
779 an Energy-Efficient Method for the Production of Nanofibrillated Cellulose at High
780 Solid Content. ACS Sustainable Chem. Eng. 5, 6524–6531.
781 https://doi.org/10.1021/acssuschemeng.7b00630
782 Rol, F., Vergnes, B., El Kissi, N., Bras, J., 2020. Nanocellulose Production by Twin-Screw
783 Extrusion: Simulation of the Screw Profile To Increase the Productivity. ACS
784 Sustainable Chem. Eng. 8, 50–59. https://doi.org/10.1021/acssuschemeng.9b01913
785 Sánchez, R., Espinosa, E., Domínguez-Robles, J., Loaiza, J.M., Rodríguez, A., 2016. Isolation
786 and characterization of lignocellulose nanofibers from different wheat straw pulps.
787 International Journal of Biological Macromolecules 92, 1025–1033.
788 https://doi.org/10.1016/j.ijbiomac.2016.08.019
789 Sauvageon, T., Lavoie, J.-M., Segovia, C., Brosse, N., 2018. Toward the cottonization of
790 hemp fibers by steam explosion – Part 1: defibration and morphological
791 characterization. Textile Research Journal 88, 1047–1055.
792 https://doi.org/10.1177/0040517517697644
793 Segal, L., Creely, J.J., Martin, A.E., Conrad, C.M., 1959. An Empirical Method for
794 Estimating the Degree of Crystallinity of Native Cellulose Using the X-Ray
795 Diffractometer. Textile Research Journal 29, 786–794.
796 https://doi.org/10.1177/004051755902901003
797 Solala, I., Iglesias, M.C., Peresin, M.S., 2020. On the potential of lignin-containing cellulose
798 nanofibrils (LCNFs): a review on properties and applications. Cellulose 27, 1853–
799 1877. https://doi.org/10.1007/s10570-019-02899-8
800 Solala, I., Volperts, A., Andersone, A., Dizhbite, T., Mironova-Ulmane, N., Vehniäinen, A.,
801 Pere, J., Vuorinen, T., 2012. Mechanoradical formation and its effects on birch kraft
802 pulp during the preparation of nanofibrillated cellulose with Masuko refining.
803 Holzforschung 66, 477–483. https://doi.org/10.1515/hf.2011.183
804 Spence, K.L., Venditti, R.A., Rojas, O.J., Habibi, Y., Pawlak, J.J., 2010. The effect of
805 chemical composition on microfibrillar cellulose films from wood pulps: water
806 interactions and physical properties for packaging applications. Cellulose 17, 835–
807 848. https://doi.org/10.1007/s10570-010-9424-8
808 Stelte, W., Sanadi, A.R., 2009. Preparation and Characterization of Cellulose Nanofibers from
809 Two Commercial Hardwood and Softwood Pulps. Ind. Eng. Chem. Res. 48, 11211–
810 11219. https://doi.org/10.1021/ie9011672
811 Sui, W., Chen, H., 2014. Multi-stage energy analysis of steam explosion process. Chemical
812 Engineering Science 116, 254–262. https://doi.org/10.1016/j.ces.2014.05.012
813 Sun, X.F., Xu, F., Sun, R.C., Geng, Z.C., Fowler, P., Baird, M.S., 2005. Characteristics of
814 degraded hemicellulosic polymers obtained from steam exploded wheat straw.
815 Carbohydrate Polymers 60, 15–26. https://doi.org/10.1016/j.carbpol.2004.11.012

Taha, M., Hassan, M., Dewidare, M., Kamel, M.A., Ali, W.Y., Dufresne, A., 2021. Evaluation of eco-friendly cellulose and lignocellulose nanofibers from rice straw using Multiple Quality Index. Egyptian Journal of Chemistry 64, 4707–4717. https://doi.org/10.21608/ejchem.2021.77618.3800

Tanahashi, M., Takada, S., Aoki, T., Goto, T., Higuchi, T., Hanai, S., 1983. <Original>Characterization of Explosion Wood : 1. Structure and Physical Properties. Wood research : bulletin of the Wood Research Institute Kyoto University 69, 36–51.

Tarrés, Q., Ehman, N.V., Vallejos, M.E., Area, M.C., Delgado-Aguilar, M., Mutjé, P., 2017. Lignocellulosic nanofibers from triticale straw: The influence of hemicelluloses and lignin in their production and properties. Carbohydrate Polymers 163, 20–27. https://doi.org/10.1016/j.carbpol.2017.01.017

Tourtollet, G., Cottin, F., Cochaux, A., Petit-Conil, M., 2003. The use of MorFi analyser to characterise mechanical pulps. pp. 225–232.

Vignon, M.R., Garcia-Jaldon, C., Dupeyre, D., 1995. Steam explosion of woody hemp chènevotte. International Journal of Biological Macromolecules 17, 395–404. https://doi.org/10.1016/0141-8130(96)81852-6

Visanko, M., Sirviö, J.A., Piltonen, P., Sliz, R., Liimatainen, H., Illikainen, M., 2017. Mechanical fabrication of high-strength and redispersible wood nanofibers from unbleached groundwood pulp. Cellulose 24, 4173–4187. https://doi.org/10.1007/s10570-017-1406-7

Wagner, W.R., Sakiyama-Elbert, S.E., Zhang, G., Yaszemski, M.J., 2020. Biomaterials Science: An Introduction to Materials in Medicine. Academic Press.

Wang, X., Cui, X., Zhang, L., 2012. Preparation and Characterization of Lignin-containing Nanofibrillar Cellulose. Procedia Environmental Sciences, The Seventh International Conference on Waste Management and Technology (ICWMT 7) 16, 125–130. https://doi.org/10.1016/j.proenv.2012.10.017

Wen, Y., Yuan, Z., Liu, X., Qu, J., Yang, S., Wang, A., Wang, C., Wei, B., Xu, J., Ni, Y., 2019. Preparation and Characterization of Lignin-Containing Cellulose Nanofibril from Poplar High-Yield Pulp via TEMPO-Mediated Oxidation and Homogenization. ACS Sustainable Chem. Eng. 7, 6131–6139. https://doi.org/10.1021/acssuschemeng.8b06355

Yousefi, H., Azari, V., Khazaeian, A., 2018. Direct mechanical production of wood nanofibers from raw wood microparticles with no chemical treatment. Industrial Crops and Products 115, 26–31. https://doi.org/10.1016/j.indcrop.2018.02.020

Yu, Z., Zhang, B., Yu, F., Xu, G., Song, A., 2012. A real explosion: The requirement of steam explosion pretreatment. Bioresource Technology 121, 335–341. https://doi.org/10.1016/j.biortech.2012.06.055

Yuan, T., Zeng, J., Wang, B., Cheng, Z., Chen, K., 2021. Lignin containing cellulose nanofibers (LCNFs): Lignin content-morphology-rheology relationships. Carbohydrate Polymers 254, 117441. https://doi.org/10.1016/j.carbpol.2020.117441

Figures and Tables list

Posidonia oceanica

Alkali-treatment

Mechanical pretreatment

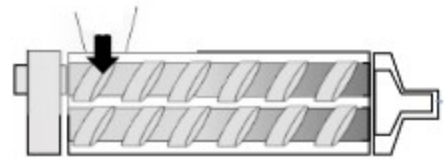

Twin-screw extrusion

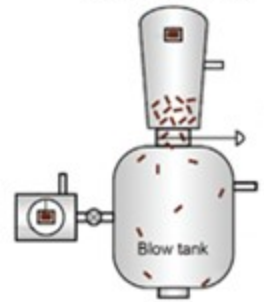

Steam explosion

Main mechanical treatment

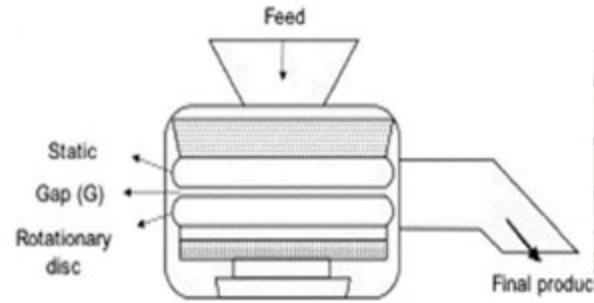

Ultra-fine grinder Masuko

LCM/NF

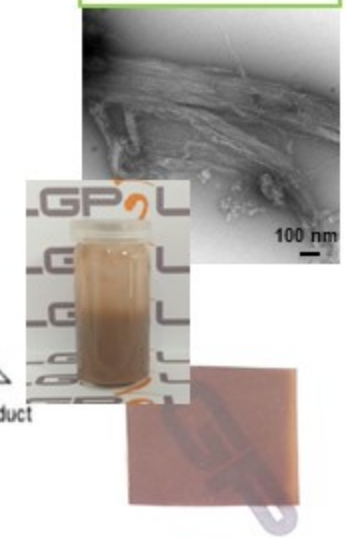

Cellulose micro/nanofibrils production